Generalizing Similarity Laws for Radio-Frequency Discharge Plasmas across Nonlinear Transition Regimes

Yangyang Fu,[1,*] Huihui Wang,[2] Bocong Zheng,[3,†] Peng Zhang,[4] Qi Hua Fan,[3,4,5] Xinxin Wang,[1] and John P. Verboncoeur[4,6]

[1] *Department of Electrical Engineering, Tsinghua University, Beijing 100084, China*
[2] *Department of Chemical Engineering, Tsinghua University, Beijing 100084, China*
[3] *Fraunhofer USA Center Midwest, Michigan State University, East Lansing, Michigan 48824, USA*
[4] *Department of Electrical and Computer Engineering, Michigan State University, East Lansing, Michigan 48824, USA*
[5] *Department of Chemical Engineering and Materials Science, Michigan State University, East Lansing, Michigan 48824, USA*
[6] *Department of Computational Mathematics, Science and Engineering, Michigan State University, East Lansing, Michigan 48824, USA*

(Received 7 July 2021; revised 24 September 2021; accepted 30 September 2021; published 8 November 2021)

We generalize similarity theory based on the scaling and solution invariance of the Boltzmann equation, coupled with the Poisson equation, and demonstrate similarity laws for radio-frequency (rf) discharge plasmas across three nonlinear transitional regimes, namely, the alpha-gamma mode transition, the stochastic-Ohmic-heating mode transition, and the bounce-resonance-heating mode transition. Fundamental plasma parameters, e.g., the electron power absorption, under similar discharge conditions are examined via fully kinetic particle-in-cell simulations, and electron-kinetic invariance is exemplified in similar rf discharge plasmas. The results unambiguously confirm the applicability of similarity laws for rf plasmas in extended operating regimes, and strengthen the foundations and framework of similarity physics with universality.

DOI: 10.1103/PhysRevApplied.16.054016

I. INTRODUCTION

Similarity laws map out how discharge conditions change in such a way that they retain the same characteristics [1–4]. They have been explored and demonstrated in discharge phenomena ranging from the laboratory to nature, such as glow discharges [5,6], streamers [7], pulsed electrical breakdown [8,9], fusion plasmas [10], and mesosphere red-sprite discharges [11,12]. The studies of similarities in gas discharges date back to those of Paschen [13] and Townsend [14], which initiated the usage of combined parameters, such as the reduced gap length pd (gas pressure times gap distance) and the reduced electric field E/p (electric field divided by gas pressure) for characterizing discharge behaviors, e.g., the use of the Townsend coefficient with a local-field approximation to describe the ionization process under a direct-current (dc) voltage. Historically, most of the initial investigations of similarity were done for dc discharges, but in 1948 Margenau [15] showed theoretically a similarity principle for high-frequency discharges. He proposed an additional combined parameter, the reduced frequency f/p (driving frequency divided by gas pressure), and this principle was later experimentally verified by Jones and Morgan [16]. In 2008, Lisovskiy *et al.* [17] experimentally validated the similarity laws for breakdown, e.g., Paschen's law [13], for radio-frequency (rf) discharges in both atomic and molecular gases, including argon, nitrogen, and hydrogen. Nowadays, due to the widespread application of rf discharge plasmas [18,19], it is of fundamental importance to elucidate the applicability of similarity laws to more comprehensive discharge regimes, and this is essential for correlating discharge parameters between rf plasma systems with different dimensional scales.

In more recent years, Puač *et al.* [20] and Lee *et al.* [21] have demonstrated breakdown similarity laws for rf discharges at macroscopic and microscopic scales, respectively. Loveless and Garner [22] conducted a nondimensionalized equation analysis of gas breakdown under rf and microwave-driven electric fields and inferred the universality of scaling laws for alternating-current gas breakdown. Very recently, rather than using a fluidic method with the local-field approximation, Fu *et al.* [23] confirmed the similarity of alpha-mode capacitive rf plasmas in nonlocal kinetic regimes through particle simulations.

*fuyangyang@tsinghua.edu.cn
†bzheng@fraunhofer.org

However, the understanding of discharge similarity laws is still far from complete; for example, to date, the effects of nonlinear physical mechanisms on discharge similarities have rarely been investigated, and the applicability of similarity laws in the discharge-mode transition regimes of rf plasmas, e.g., the alpha-gamma (AG) mode transition [24], the stochastic-Ohmic (SO)-heating mode transition [25,26], and the bounce-resonant-heating (BRH) mode transition [27–29], has not yet been confirmed, which severely limits the application of similarity theory.

In this paper, we generalize the similarity laws for rf discharge plasmas across the three aforementioned nonlinear transition regimes, i.e., the AG, SO, and BRH mode transitions. Based on fully kinetic particle-in-cell (PIC) and Monte Carlo collision simulations, the AG, SO, and BRH mode transitions are observed in rf plasmas by tuning the applied rf voltage, the gas pressure, and the gap distance, respectively, showing distinctive nonlinear parameter-scaling relations. By simultaneously manipulating the external discharge-condition parameters $[p, d, f]$, we find that the nonlinear characteristics can be exactly replicated under similar discharge conditions, which unambiguously confirms the validity of the similarity laws across the nonlinear transition regimes considered. The results of the present work provide additional knobs and more flexibility for characterizing rf discharges across a wider range of parameter regimes, which is essential for the optimization and fabrication of plasma devices.

II. THEORY AND MODEL

Similarity laws are usually utilized for the correlation of discharges in geometrically similar gaps, the linear dimensions of which are proportional in every direction, i.e., $d_{1j} = kd_{kj}$, where $j = [x, y, z]$ represents the coordinate direction, d_1 is the dimension in the base (or prototype) case, and d_k is the dimension in a scaled case that, compared with the base case, has a geometrical scaling factor of k. According to similarity theory [30], a physical parameter $G(x, t)$ at the corresponding spatiotemporal points (x, t) in similar discharge systems can be transformed through

$$G(x_1, t_1) = k^{\alpha[G]} G(x_k, t_k), \tag{1}$$

where the subscripts 1 and k indicate the prototype gap and the scaled gap, which has a scaling factor of k, respectively; (x_1, t_1) and (x_k, t_k) are the corresponding spatiotemporal points in the gaps being compared, which are defined by the scaling factor $k = x_1/x_k = t_1/t_k$; and $\alpha[G]$ is the similarity factor for the parameter G. Note that the scaling factor k need not be an integer and can be less than one. The most common similarity factors include $\alpha[n_e] = \alpha[\mathbf{J}_e] = -2$ for the electron density n_e and electron current density $\mathbf{J}_e$, $\alpha[\mathbf{E}] = \alpha[p] = -1$ for the electric field $\mathbf{E}$ and gas pressure p, $\alpha[\varepsilon_e] = \alpha[\mathbf{v}_e] = 0$ for the electron energy ε_e and electron velocity $\mathbf{v}_e$, and $\alpha[d] = \alpha[x] = \alpha[t] = 1$ for the gap dimension d, position x, and time t [31]. In particular, from the transformation in Eq. (1), the parameters having $\alpha[G] = 0$ are similarity invariants, such as the combined parameters E/p and n_e/p^2 [32].

Previously, similarity theory has mostly been developed within the framework of local-field or local-energy approximations [15,33]. However, in low-pressure rf discharges, the electron kinetics can be highly nonlocal, and the local reduced electric field may not be proportional to the mean electron energy, which is a prerequisite for the conventional explanations. Here, in the following, we interpret the similarity laws using a more generalized approach, which is based on the scaling and solution invariance of the Boltzmann equation, coupled with the Poisson equation. Considering rf plasmas in weakly ionized regimes, the collisions are dominated by electron-neutral collisions, and the Boltzmann equation for the electrons can be expressed as

$$\frac{\partial f_e}{\partial t} + \mathbf{v} \cdot \nabla_{\mathbf{x}} f_e - \frac{e\mathbf{E}}{m_e} \cdot \nabla_{\mathbf{v}} f_e = \sum_j C_{en}^j [f_e f_n, v_{en}, \sigma_{en}(v_{en})], \tag{2}$$

where f_e is the electron distribution function, $\mathbf{v}$ is the velocity, e is the elementary charge, and $C_{en}^j[f_e f_n, v_{en}, \sigma_{en}(v_{en})]$ is an integral term for the jth collision between electrons and neutrals, which depends on the relative velocity v_{en}, the collision cross section $\sigma_{en}(v_{en})$, and the distributions of electrons and neutrals f_e and f_n [34]. By dividing Eq. (2) by k^3, we have

$$\frac{\partial (f_e/k^2)}{\partial (kt)} + \mathbf{v} \cdot \nabla_{(k\mathbf{x})} (f_e/k^2) - \frac{e(\mathbf{E}/k)}{m_e} \cdot \nabla_{\mathbf{v}} (f_e/k^2) = \sum_j C_{en}^j [(f_e/k^2)(f_n/k), v_{en}, \sigma_{en}(v_{en})]. \tag{3}$$

Note that once the systems to be compared are given, k is a constant and can be put inside the integration of the collision term. By substituting the scaled parameters, i.e., kt, $k\mathbf{x}$, $\mathbf{E}/k$, f_n/k, and f_e/k^2, Eqs. (2) and (3) can be used to demonstrate solution invariance. Considering Eq. (2) for the base case and Eq. (3) for the scaled system, one can rewrite the parameter relation using Eq. (1) and then obtain $\alpha[t] = \alpha[\mathbf{x}] = 1$, $\alpha[\mathbf{E}] = -1$, $\alpha[f_n] = -1$, and $\alpha[f_e] = -2$, which consistently explains the scaling factors for different parameters.

Note that for more detailed descriptions of the collision term, one needs to refer to the Boltzmann collision integral or the Fokker-Planck collision term [35]. Since the main collisional processes in a weakly ionized plasma are between charged and neutral particles, the simultaneous Coulomb interactions between charged particles are not taken into account here and are beyond the scope of the

present work. Therefore, we employ a Krook-like relaxation model [35] that can be derived from the simplified Boltzmann collision integral, assuming that the neutral distribution f_n is stationary and not perturbed by collisions. The relaxation model for the collision term is expressed as $(\delta f_e/\delta t)_{\rm coll} = -\nu_{\rm rc}(f_e - f_{e0})$, where $\nu_{\rm rc} = \sigma_m v_{en} N_n \propto p$ is the velocity-dependent relaxation-collision frequency, with σ_m being the momentum-transfer cross section and N_n the number density of neutral particles in the gas, and f_{e0} is the equilibrium distribution function of the electrons. In Eq. (3), when the collision term is divided by k^3, since $\alpha[\nu_{\rm rc}] = \alpha[p] = -1$, $\alpha[f_e] = \alpha[f_{e0}] = -2$ can be directly concluded from the solution invariance of the equation. Although the collision term for the interparticle interactions is simplified, the general idea of the similarity scalings can be straightforwardly demonstrated in a kinetic manner.

From $\alpha[f_e] = -2$ and $n_e = \int f_e(\mathbf{v})\, d\mathbf{v}$, we can directly obtain the similarity factor for the electron density, $\alpha[n_e] = -2$. Further, we can also identify the similarity scaling for the Poisson equation, which is expressed as $-\partial(\varepsilon \mathbf{E})/\partial x = e\int [f_e(\mathbf{v}) - f_i(\mathbf{v})]\, d\mathbf{v}$, with ε being the permittivity constant. Here, $\alpha[\partial \mathbf{E}/\partial x] = \alpha[\mathbf{E}] - \alpha[x] = -2$ is equal to $\alpha[f_i] = \alpha[f_e] = -2$, which indicates that the Poisson equation also follows the similarity scaling. Similarly, for the electron current density, the scaling factor is $\alpha[\mathbf{J}_e] = \alpha[n_e] + \alpha[\mathbf{v}_e] = -2$, where $\alpha[n_e] = -2$ and $\alpha[\mathbf{v}_e] = 0$; this is also the case for the ion and total current densities, i.e., $\alpha[\mathbf{J}_i] = \alpha[\mathbf{J}_{\rm tot}] = -2$. Further, for rf discharge plasmas, since $\alpha[f] = \alpha[1/t] = -1$, the external driving frequency f needs to be tuned to keep the solution invariance, which indicates that the reduced frequency f/p needs to be constant, or is a similarity invariant in the systems being compared, i.e., $\alpha[f/p] = 0$. Here, mathematically, the similarity theory is self-consistently interpreted on the basis of the Boltzmann and Poisson equations with universality, which can be applied to rf discharge plasmas.

A schematic illustration of two similar discharge systems (S, S^s) having different dimensional scales is shown in Fig. 1(a), where $G(x,t)$ is a physical parameter at the corresponding spatiotemporal points. We hereby make a statement to distinguish between similarity and scaling laws. The former hold with multiple control parameters scaled simultaneously, e.g., if the similarity invariants pd and f/p are maintained to achieve similar rf discharges. The later usually determine the dependence of the discharge parameters on only one of the controlled parameters, e.g., the scaling of the discharge characteristics with the gas pressure [36,37], gap dimension [38,39], and driving frequency [40]. As illustrated in Fig. 1(b), the scaling laws establish the dependence of plasma parameters from S_1 to S_n [or from S_1^s to S_n^s], whereas the similarity laws correlate plasmas between (S_1, S_n) and (S_1^s, S_n^s). Strategically, if the similarity laws are valid, discharge properties for S can be directly applied to S^s and vice versa; thus the conventional scaling laws can be exactly extrapolated from one system to another, enabling extended parameter regimes for prediction in various rf plasma systems.

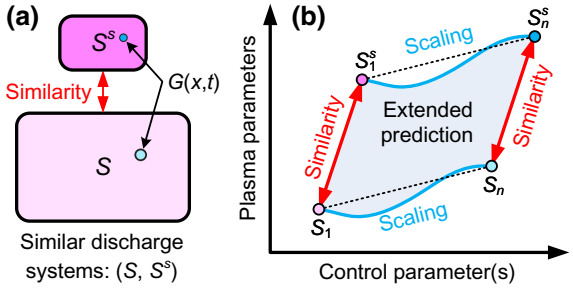

FIG. 1. (a) Schematic illustration of similar discharge systems (S, S^s) with different dimensional scales. (b) A strategy for showing that plasma properties can be predicted in an extended range of parameter regimes by combining both the scaling and the similarity laws.

In the following, PIC simulations are employed to demonstrate the applicability of the similarity laws for rf discharge plasmas across the AG, SO, and BRH nonlinear transition regimes. The simulations of the rf plasmas are performed for argon at 300 K, accounting for three types of electron-neutral collisions (elastic, excitation, and ionization scattering) and two types of ion-neutral collisions (isotropic and backward scattering) [41]. A custom-developed electrostatic PIC code, ASTRA, is used for all the simulations (see [42] for the code benchmark with the results from Turner *et al.* [43] and other details). Argon ions and electrons are tracked as particles. The rf plasmas are geometrically symmetric between two parallel-plate electrodes for simplicity. The rf voltage waveform $V_{\rm rf}(t) = V_{\rm rf}\sin(2\pi f t)$ (in units of volts), where $f = 1/T$ is the driving frequency, with T being the rf period, is connected to the powered electrode ($x = 0$), while the other electrode ($x = d$) is grounded. To satisfy the requirement for similar discharge conditions, the gas pressure p, gap distance d, and driving frequency f are simultaneously tuned with respect to the scaling factor k, i.e., $k = p_k/p_1 = d_1/d_k = f_k/f_1$, keeping f/p and pd constant in the systems being compared. The emission coefficient of the ion-induced secondary electron is $\gamma_{\rm se} = 0.1$ when it is considered, and the electron reflection probability is $\gamma_{\rm re} = 0.2$ in all cases [44]. In the simulations, an implicit algorithm and an energy-conservation scheme are adopted; the grid number and time step are case dependent, while most of the cases have 300 grid points and 2000 time steps per rf period.

III. RESULTS AND DISCUSSION

We demonstrate similarity in rf discharges during the AG mode transition in Fig. 2. In the simulations, we set $[p, d, f] = [0.3\ \text{Torr}, 6.7\ \text{cm}, 13.56\ \text{MHz}]$ in S and

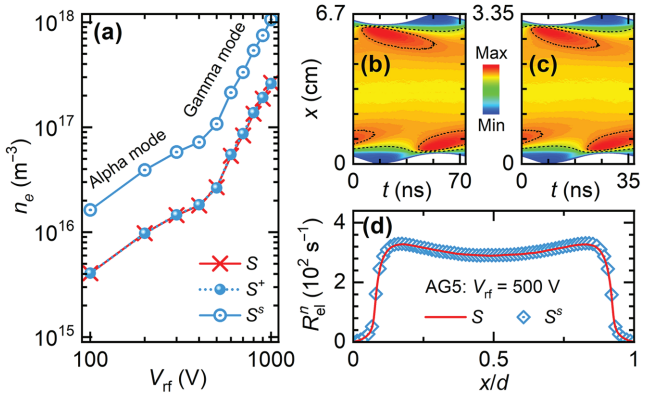

FIG. 2. (a) Bulk electron density versus $V_{\rm rf}$ under similar discharge conditions during the AG mode transition. In the simulations, we set $[p,d,f] = [0.3\ \text{Torr}, 6.7\ \text{cm}, 13.56\ \text{MHz}]$ for S and $[p,d,f] = [0.6\ \text{Torr}, 3.35\ \text{cm}, 27.12\ \text{MHz}]$ for S^s with $\gamma_{\rm se} = 0.1$. Taking $V_{\rm rf} = 500$ V (case AG5) as an example to demonstrate the dynamical similarities, (b),(c) spatiotemporal distributions of the elastic-collision rates normalized to their maxima in S and S^s, respectively; (d) time-averaged scaled rates across the gap.

$[p,d,f] = [0.6\ \text{Torr}, 3.35\ \text{cm}, 27.12\ \text{MHz}]$ in S^s, with a scaling factor $k = 2$, and have $\gamma_{\rm se} = 0.1$ in all cases. The AG mode transitions are obtained by varying $V_{\rm rf}$ from 100 to 1000 V, i.e., we have ten cases AG1–AG10 in S and S^s [see Fig. 2(a)]. The transition occurs around a critical voltage $V_{\rm rf} = 500$ V, before and after which the time-averaged bulk electron density n_e versus $V_{\rm rf}$ shows two distinctly different scaling laws. The slope in the gamma mode is much higher than that in the alpha mode, which is also consistent with the experimental results of Godyak *et al.* [24] and the simulation results of Belenguer and Boeuf [45]. Most importantly, the electron-density scaling S^+, which is extrapolated from S^s using n_e/k^2, can be superimposed on that in S. This indicates that the AG mode transition, though nonlinear, can be exactly replicated from one system to another. The spatiotemporal distributions of the electron-neutral elastic-collision rate, $R_{\rm el} = K_{\rm el} n_e N_n$, where $K_{\rm el}$ is the reaction-rate coefficient, normalized to their maxima in S and S^s for $V_{\rm rf} = 500$ V (case AG5), are found to be the same [see Figs. 2(b) and 2(c)]. It is confirmed that the similarities hold in a dynamical manner with the time domain scaled correspondingly. The corresponding time-averaged scaled reaction rates normalized to the gas number density, i.e., $R^n_{\rm el} = k^{-2} R_{\rm el} N_n^{-1}$, are also exactly the same in S and S^s [see Fig. 2(d)], which explicitly confirms that $\alpha[R^n_{\rm el}] = \alpha[n_e] = -2$ and quantitatively validates the similarity laws for the rf plasma systems being compared.

A study of the power absorption by electrons (or electron heating), which is a widely studied phenomenon, is essential for a deep understanding of the fundamental behavior of rf discharge plasmas. The electron power absorption can be expressed as $P_e = \mathbf{J}_e \cdot \mathbf{E}$, and, according to the previous discussion, we have $\alpha[P_e] = \alpha[\mathbf{J}_e] + \alpha[\mathbf{E}] = -3$, which indicates that $k^{-3}P_e$ should be invariant in similar rf discharges. It is generally considered that low-pressure rf plasmas are maintained by stochastic heating, while at higher pressures the dominant heating process is Ohmic, and thus the SO mode transition can be observed by tuning the gas pressure [19]. Note that stochastic heating has previously been called collisionless heating, which may not be accurate. According to studies [46–48] in more recent years, it has been recognized that collisions are needed to break the phase coherence between the electron motion and the rf electric field, resulting in net heating during one rf cycle, and at low pressures this occurs by nonlocal collisions, whereby collisions occur at a different spatial location from where the energy gain occurs from the rf fields. Therefore, more exactly, the conventional collisionless heating should be understood as nonlocal collisional heating, also known as pressure heating. In the PIC simulations, the SO mode transition in the heating mechanism is observed at different pressures; meanwhile, the applicability of the similarity laws for the rf plasma is examined.

We run seven pressure-dependent cases (SO1–SO7) in the range $p/k = 0.01$–1 Torr, with $k = 1$ in S and $k = 2$ in S^s. It is observed that the electron density n_e increases as the gas pressure p increases, with $V_{\rm rf} = 300$ V and $\gamma_{\rm se} = 0.1$ used in all cases. Figure 3 shows the similarity of the discharges when the dominant electron power absorption transitions from stochastic to Ohmic heating. The overlapping of the scaled electron-density curves, S^+ and S, confirms the validity of the similarity factor $\alpha[n_e] = -2$ [see Fig. 3(a)] during the SO transition. To further examine the electron heating mode, we decompose the electron power absorption P_e into the stochastic heating $P_{e,\rm st}$ and the Ohmic heating $P_{e,\rm Ohm}$, i.e., $P_e = P_{e,\rm st} + P_{e,\rm Ohm}$, based on a moment analysis of the electron Boltzmann equation [46,48–50]. The $P_{e,\rm Ohm}/P_{e,\rm st}$ ratios in S and S^s are shown in Fig. 3(b), which unambiguously demonstrates that the transitions from stochastic to Ohmic heating with increasing gas pressure overlap in similar discharge systems (S, S^s). We take two cases, with $p/k = 0.01$ Torr (SO1) and $p/k = 1$ Torr (SO7), as examples to further confirm the similarity in the spatial distribution of the electron power absorption. In Fig. 3(c), the scaled electron power absorption, $k^{-3}P_e$, at 0.01 Torr in S and 0.02 Torr in S^s are the same, with the dominant electron heating rate being stochastic within the averaged sheath and the bulk Ohmic heating being negligible. Figure 3(d) shows the same scaled total electron power absorption in SO7, i.e., at 1 Torr in S and 2 Torr in S^s, with the Ohmic heating being dominant. In comparison with Fig. 3(c), the magnitudes of the electron heating rate are greatly increased, and there is significant positive electron heating in the bulk region. Figure 3(e) presents the decomposed electron heating rates corresponding to Fig. 3(d), with, correspondingly, the same scaled stochastic

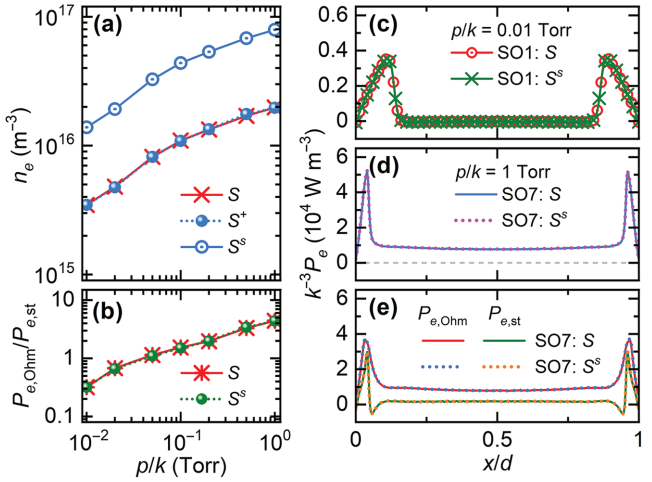

FIG. 3. Similarity of discharges in rf plasmas with an electron-heating transition from the stochastic to the Ohmic regime. (a) Bulk electron density and (b) corresponding ratio between the Ohmic and stochastic heating components in similar discharge systems with p/k from 0.01 to 1 Torr. Time-averaged spatial distributions of the electron heating rate at (c) $p/k = 0.01$ Torr (SO1, stochastic-heating-dominated) and (d) $p/k = 1$ Torr (SO7, Ohmic-heating-dominated). (e) Decomposition of the electron heating rate in S and S^s at $p/k = 1$ (SO7). In the simulations, we have $V_{\mathrm{rf}} = 300$ V and $\gamma_{\mathrm{se}} = 0.1$ in all cases, and set $[d,f] =$ [6.7 cm, 13.56 MHz] in S and $[d,f] = [3.35$ cm, 27.12 MHz] in S^s.

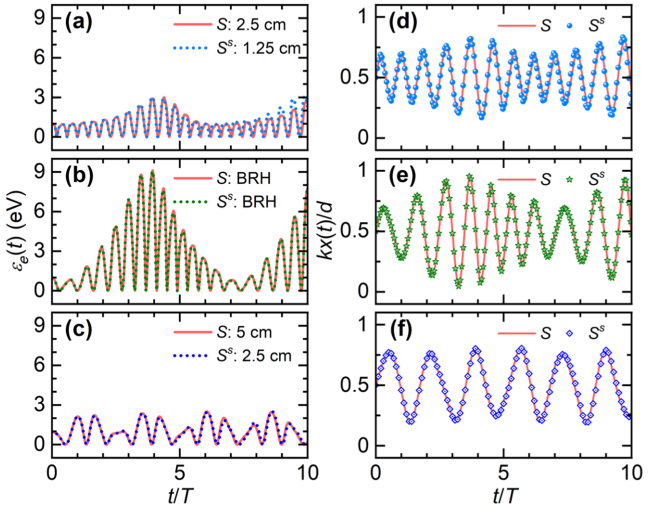

FIG. 4. Determining the BRH mode transition by tuning the gap distance using test-particle simulations. The gap distances are (a) (2.5, 1.25), (b) (4.5, 2.25) (under the BRH condition), and (c) (5 cm, 2.5 cm) in (S, S^s). (d)–(f) Spatiotemporal electron trajectories corresponding to (a)–(c). In the simulations, we have $[p,f] = [0.025$ Torr, 13.56 MHz] in S and $[p,f] =$ [0.05 Torr, 27.12 MHz] in S^s, with $V_{\mathrm{rf}} = 40$ V and secondary electrons neglected ($\gamma_{\mathrm{se}} = 0$) in all cases.

and Ohmic heating components in S and S^s. Note also that $P_{e,\mathrm{Ohm}} > P_{e,\mathrm{st}}$ holds across the gap. Thus the similarity laws apply to rf plasmas dominated by either stochastic or Ohmic heating, as well as in the transition regime.

Under certain conditions, electrons can be bounced back and forth many times between rf sheath fields and continuously accelerated without experiencing collisions; the discharge is then operating in the BRH mode, which is considered as a typical nonlinear mechanism in rf plasmas [27–29]. Here we examine the BRH nonlinear transition with $V_{\mathrm{rf}} = 40$ V and $\gamma_{\mathrm{se}} = 0$ under similar discharge conditions. The discharge-condition parameters are $[p,f] = [0.025$ Torr, 13.56 MHz] in S and $[p,f] =$ [0.05 Torr, 27.12 MHz] in S^s. The BRH mode transitions are identified by tuning the gap distance, i.e., $d =$ (2.5, 1.25), (4.5, 2.25), and (5 cm, 2.5 cm) for (S, S^s). The temporal evolution of the electron kinetic energy $\varepsilon_e(t)$ obtained from test-particle simulations is shown in Figs. 4(a)–4(c), which demonstrate a gradual transition across the BRH mode. The test-particle simulations are conducted using spatiotemporal electric fields obtained from PIC simulations of the rf discharges in the steady state. Under the BRH condition [see Fig. 4(b)], the electron energy is highly enhanced, up to 9 eV, whereas $\varepsilon_e(t)$ is generally less than 3 eV when BRH is less significant [see Figs. 4(a) and 4(c)]. Note that the efficiency of the BRH mode demonstrated here is even higher than that obtained by Park *et al.* [27], since the discharge-condition parameters in the BRH mode are further optimized. Although the BRH mode and its transition are considered to be nonlinear, this phenomenon can actually be reproduced in similar discharge systems. The corresponding normalized trajectories of the test particles, $kx(t)/d$, where $x(t)$ is the temporal position of the test particle, also overlap in S and S^s [see Figs. 4(d)–4(f)], which ensures the applicability of similarity laws in the rf plasmas during the BRH mode transition.

Further, we examine the behavior of the electron kinetics in rf plasmas under similar discharge conditions. As mentioned before, we have $\alpha[f_e/n_e] = \alpha[f_e] - \alpha[n_e] = 0$ in similar discharges, and thus the normalized electron distribution function f_e/n_e should be an invariant. Converting f_e to the normalized electron energy probability function (EEPF) f_p using $\sqrt{\varepsilon} f_p(\varepsilon)\, d\varepsilon = 4\pi \mathbf{v}^2 f_e(\mathbf{v})\, d\mathbf{v}/n_e$, we have $\alpha[f_p] = \alpha[f_e/n_e] = 0$ from Eq. (1), from which we conclude that the EEPF is also invariant. The temporal and time-averaged EEPFs in the full space under various similar discharge conditions are shown in Fig. 5. In Figs. 5(a)–5(c), we show the temporal EEPFs in (a) the alpha mode with $V_{\mathrm{rf}} = 100$ V (AG1), (b) the stochastic-heating-dominated mode with $p/k = 0.01$ Torr (SO1), and (c) the BRH mode with a gap length of 4.5 cm in S. Figures 5(d)–5(f) show the corresponding EEPFs in S^s under similar discharge conditions. Although the EEPFs in different discharge modes are quite different,

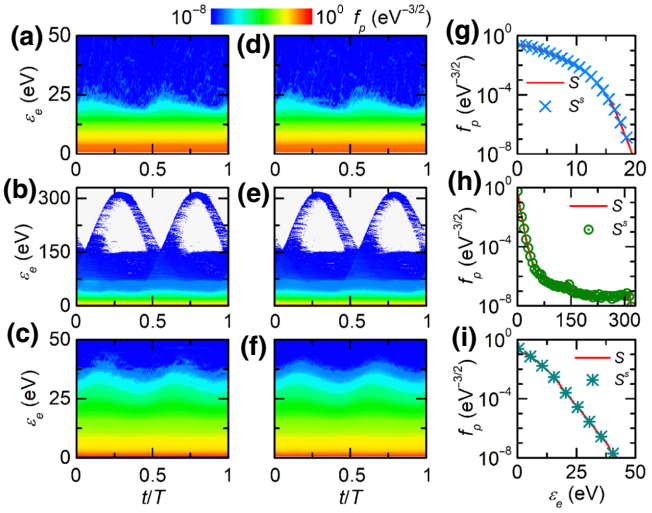

FIG. 5. Invariance of electron kinetics under similar discharge conditions. Temporal EEPFs in full space corresponding to (a) AG1, (b) SO1, (c) BRH in S and (d) AG1, (e) SO1, (f) BRH in S^s. (g)–(i) Time-averaged EEPFs in S and S^s under similar discharge conditions.

the distributions are the same in similar discharge systems. Figures 5(g)–5(i) show the time-averaged EEPFs in S and S^s, which further confirm the invariance of the electron kinetics in similar discharges. It is also noteworthy that in Figs. 5(b) and 5(e) the wavy trajectories are due to secondary electrons, which have been characterized as high-energy ballistic electrons [51]. These electrons are accelerated across the sheath ballistically and obtain the full potential energy, which is converted to the kinetic energy, and their maximum energy is close to the gap voltage ($V_{\rm rf} = 300$ V) plus the plasma potential. Here the invariance of the electron kinetics, holding for electrons from different energy groups, is of fundamental importance, which guarantees the similarity laws under various discharge conditions.

Our results confirm that the nonlinear transition behaviors in rf plasmas can be exactly replicated under similar discharge conditions by simultaneously tuning the external discharge parameters $[p, d, f]$, keeping pd and f/p constant in the systems being compared. Physically, $pd \propto d/\lambda \sim N_{\rm coll}$ (where λ is the mean free path) represents the electron mean collision number across the gap, and $f/p \propto f/\nu_{\rm coll} = T^{-1}/\tau_{\rm coll}^{-1} \sim N_{\rm coll}^{-1}$ (where $\nu_{\rm coll} = \tau_{\rm coll}^{-1} \propto p$ is the electron collision frequency) indicates the inverse of the electron mean collision number during one rf cycle. Since pd and f/p are kept constant under similar discharge conditions, $fd = pd \times f/p$ is also maintained; this is a well-known similarity parameter for multipactor discharges, which usually occur in vacuum or at rather low pressures, where the pressure effect is not typically considered [17,52]. The three combined parameters are not independent, and any two of them can be chosen and can function equivalently; here pd and f/p are selected, since the pressure effect is critical for rf discharge plasmas. Although the kinetic interpretations are no longer based on local-field approximations, the reduced electric field E/p is still a similarity invariant here, and this holds for the separated electric field components, e.g., the electrostatic field and the space-charge field, as well as the total electric field, in similar rf discharges. The idea of similarity scalings is essentially similar to the Buckingham π theorem [53], and both of these can be used to reduce the number of independent parameters required for describing physically similar systems [5]. We would like to further emphasize that the similarity laws are more useful for extrapolating discharge parameters among similar discharge systems, whereas the π theorem is also typically utilized for dimensional analysis.

In the present paper, similarity laws are demonstrated for a scaling factor $k = 2$ and a one-dimensional geometry. Similarity properties are also expected for larger scaling factors and for higher-dimensional geometrically similar systems when the fundamental physical processes are maintained. For example, similar rf discharges can still be obtained in systems being compared for $k = 10$ [31]. However, for larger values of k, the scaled rf discharge parameters may enter high-pressure and high-ionization-degree regimes, in which other collision processes (e.g., stepwise ionization and Coulomb collisions [54]) could be important, and their effects need further investigation. Also, currently the results are for atomic gases only, and the scaling laws could be more complicated for electronegative or molecular gases, since negative ions and ion-ion recombination should be additionally considered.

IV. CONCLUSION

We generalize and demonstrate similarity laws for rf plasmas across various nonlinear transition regimes, based on theoretical interpretations and fully kinetic particle simulations. From the perspective of similarity theory, the nonlinear transition behaviors, such as the AG, SO, and BRH mode transitions, can be exactly replicated in similar discharge systems, and thus the scaling laws during the transitions can be extrapolated from one system to another. The fundamental mechanisms, such as the invariance of the electron kinetics, that maintain the similarity laws are elucidated based on the scaling and solution invariance of the Boltzmann equations and the coupled Poisson equation. The results of the present work bring comprehensive insights and additional flexibility to plasma characterization in extended parameter regimes, and provide valuable guidance for developing upscaled plasma devices, e.g., next-generation plasma-processing facilities for etching applications. Moreover, the generalization of the similarity laws also suggests a strategy for scale

reduction in large-scale simulations when the model equations can be treated as absolute invariants. The effects of stepwise ionization at high pressures, Coulomb collisions in highly ionized regimes, and possible electromagnetic mechanisms [55,56] at high frequencies, as well as the applicability of the similarity laws to discharge plasmas in electronegative gases [57–59], will be explored in future work.

ACKNOWLEDGMENTS

This work is supported by the State Key Laboratory of Power System and Generation Equipment at Tsinghua University, Project No. SKLD21M06. B.Z. and Q.H.F. acknowledge funding support from the National Science Foundation, Grants No. 1917577 and No. 1724941, in the United States. J.P.V. acknowledges funding support from the U.S. Department of Energy Office of Fusion Energy Science, Grant No. DE-SC0001939. P.Z. acknowledges funding support from the Air Force Office of Scientific Research, YIP Grant No. FA9550-18-1-0061. J.P.V. and P.Z. also acknowledge funding support from the Air Force Office of Scientific Research, Grant No. FA9550-18-1-0062 and the U.S. Department of Energy Office of Science, Grant No. DE-SC0022078.

Y.F. and H.W. contributed equally to this work.

[1] D. Janasek, J. Franzke, and A. Manz, Scaling and the design of miniaturized chemical-analysis systems, Nature **442**, 374 (2006).

[2] D. D. Ryutov, Scaling laws for dynamical plasma phenomena, Phys. Plasmas **25**, 100501 (2018).

[3] Y. Fu and J. P. Verboncoeur, On the similarities of low-temperature plasma discharges, IEEE Trans. Plasma Sci. **47**, 1994 (2019).

[4] J. P. Sauppe, S. Palaniyappan, B. J. Tobias, J. L. Kline, K. A. Flippo, O. L. Landen, D. Shvarts, S. H. Batha, P. A. Bradley, E. N. Loomis, N. N. Vazirani, C. F. Kawaguchi, L. Kot, D. W. Schmidt, T. H. Day, A. B. Zylstra, and E. Malka, Demonstration of Scale-Invariant Rayleigh-Taylor Instability Growth in Laser-Driven Cylindrical Implosion Experiments, Phys. Rev. Lett. **124**, 185003 (2020).

[5] D. Michael, M. Khodorkovskii, A. Pastor, N. Timofeev, and G. Zissis, Application of similarity laws as a light source diagnostics, J. Phys. D: Appl. Phys. **43**, 234005 (2010).

[6] A. von Engel, *Ionized Gases* (Clarendon, Oxford, 1965).

[7] T. M. P. Briels, E. M. Van Veldhuizen, and U. Ebert, Positive streamers in air and nitrogen of varying density: Experiments on similarity laws, J. Phys. D: Appl. Phys. **41**, 234008 (2008).

[8] G. A. Mesyats, Similarity laws for pulsed gas discharges, Phys.-Usp. **49**, 1045 (2006).

[9] P. Osmokrović, T. Živić, B. Lončar, and A. Vasić, The validity of the general similarity law for electrical breakdown of gases, Plasma Sources Sci. Technol. **15**, 703 (2006).

[10] C. C. Petty, Sizing up plasmas using dimensionless parameters, Phys. Plasmas **15**, 080501 (2008).

[11] N. Liu and V. P. Pasko, Effects of photoionization on similarity properties of streamers at various pressures in air, J. Phys. D: Appl. Phys. **39**, 327 (2006).

[12] V. P. Pasko, Red sprite discharges in the atmosphere at high altitude: The molecular physics and the similarity with laboratory discharges, Plasma Sources Sci. Technol. **16**, S13 (2007).

[13] F. Paschen, Ueber die zum Funkenübergang in Luft, Wasserstoff und Kohlensäure bei verschiedenen Drucken erforderliche Potentialdifferenz, Ann. Phys. **273**, 69 (1889).

[14] J. S. Townsend, *Electricity in Gases* (Clarendon, Oxford, 1915).

[15] H. Margenau, Theory of high frequency gas discharges. IV. Note on the similarity principle, Phys. Rev. **73**, 326 (1948).

[16] F. L. Jones and G. D. Morgan, High-frequency discharges: I breakdown mechanism and similarity relationship, Proc. Phys. Soc. Lond. B **64**, 560 (1951).

[17] V. Lisovskiy, J. P. Booth, K. Landry, D. Douai, V. Cassagne, and V. Yegorenkov, Similarity law for rf breakdown, Europhys. Lett. **82**, 15001 (2008).

[18] M. A. Lieberman and A. J. Lichtenberg, *Principles of Plasma Discharges and Materials Processing* (John Wiley & Sons, New York, 2005).

[19] P. Chabert and N. Braithwaite, *Physics of Radio-Frequency Plasmas* (Cambridge University Press, Cambridge, 2011).

[20] M. Puač, D. Marić, M. Radmilović-Radjenović, M. Šuvakov, and Z. L. Petrović, Monte Carlo modeling of radio-frequency breakdown in argon, Plasma Sources Sci. Technol. **27**, 075013 (2018).

[21] M. U. Lee, J. Lee, J. K. Lee, and G. S. Yun, Extended scaling and Paschen law for micro-sized radiofrequency plasma breakdown, Plasma Sources Sci. Technol. **26**, 034003 (2017).

[22] A. M. Loveless and A. L. Garner, Scaling laws for AC gas breakdown and implications for universality, Phys. Plasmas **24**, 104501 (2017).

[23] Y. Fu, B. Zheng, D.-Q. Wen, P. Zhang, Q. H. Fan, and J. P. Verboncoeur, Similarity law and frequency scaling in low-pressure capacitive radio frequency plasmas, Appl. Phys. Lett. **117**, 204101 (2020).

[24] V. A. Godyak, R. B. Piejak, and B. M. Alexandrovich, Measurement of electron energy distribution in low-pressure rf discharges, Plasma Sources Sci. Technol. **1**, 36 (1992).

[25] I. D. Kaganovich, V. I. Kolobov, and L. D. Tsendin, Stochastic electron heating in bounded radio-frequency plasmas, Appl. Phys. Lett. **69**, 3818 (1996).

[26] M. M. Turner and P. Chabert, Collisionless Heating in Capacitive Discharges Enhanced by Dual-Frequency Excitation, Phys. Rev. Lett. **96**, 205001 (2006).

[27] G. Y. Park, S. J. You, F. Iza, and J. K. Lee, Abnormal Heating of Low-Energy Electrons in Low-Pressure Capacitively Coupled Discharges, Phys. Rev. Lett. **98**, 085003 (2007).

[28] Y.-X. Liu, Q.-Z. Zhang, W. Jiang, L.-J. Hou, X.-Z. Jiang, W.-Q. Lu, and Y.-N. Wang, Collisionless Bounce Resonance Heating in Dual-Frequency Capacitively Coupled Plasmas, Phys. Rev. Lett. **107**, 055002 (2011).

[29] T. Mussenbrock, R. P. Brinkmann, M. A. Lieberman, A. J. Lichtenberg, and E. Kawamura, Enhancement of Ohmic and Stochastic Heating by Resonance Effects in Capacitive

Radio Frequency Discharges: A Theoretical Approach, Phys. Rev. Lett. **101**, 085004 (2008).
[30] A. A. Rukhadze, N. N. Sobolev, and V. V. Sokovikov, Similarity relations for low-temperature nonisothermal discharges, Sov. Phys. Usp. **34**, 827 (1991).
[31] Y. Fu, B. Zheng, P. Zhang, Q. H. Fan, J. P. Verboncoeur, and X. Wang, Similarity of capacitive radio-frequency discharges in nonlocal regimes, Phys. Plasmas **27**, 113501 (2020).
[32] F. Iza, J. K. Lee, and M. G. Kong, Electron Kinetics in Radio-Frequency Atmospheric-Pressure Microplasmas, Phys. Rev. Lett. **99**, 075004 (2007).
[33] G. J. M. Hagelaar and L. C. Pitchford, Solving the Boltzmann equation to obtain electron transport coefficients and rate coefficients for fluid models, Plasma Sources Sci. Technol. **14**, 722 (2005).
[34] C. E. Muehe, Scaling laws for high-density plasmas, J. Appl. Phys. **45**, 82 (1974).
[35] J. A. Bittencourt, *Fundamentals of Plasma Physics* (Springer Science & Business Media, New York, 2004).
[36] M. Vass, S. Wilczek, T. Lafleur, R. P. Brinkmann, Z. Donkó, and J. Schulze, Observation of dominant ohmic electron power absorption in capacitively coupled radio frequency argon discharges at low pressure, Plasma Sources Sci. Technol. **29**, 085014 (2020).
[37] Y. Fu, P. Zhang, J. P. Verboncoeur, and X. Wang, Electrical breakdown from macro to micro/nano scales: A tutorial and a review of the state of the art, Plasma Res. Express **2**, 013001 (2020).
[38] K. Bera, S. Rauf, K. Ramaswamy, and K. Collins, Effects of interelectrode gap on high frequency and very high frequency capacitively coupled plasmas, J. Vac. Sci. Technol. A **27**, 706 (2009).
[39] A. M. Loveless and A. L. Garner, Scaling laws for gas breakdown for nanoscale to microscale gaps at atmospheric pressure, Appl. Phys. Lett. **108**, 234103 (2016).
[40] S. Sharma, N. Sirse, M. M. Turner, and A. R. Ellingboe, Influence of excitation frequency on the metastable atoms and electron energy distribution function in a capacitively coupled argon discharge, Phys. Plasmas **25**, 063501 (2018).
[41] B. Zheng, Y. Fu, D. Q. Wen, K. Wang, T. Schuelke, and Q. H. Fan, Influence of metastable atoms in low pressure magnetized radio-frequency argon discharges, J. Phys. D: Appl. Phys. **53**, 435201 (2020).
[42] B. Zheng, K. Wang, T. Grotjohn, T. Schuelke, and Q. H. Fan, Enhancement of ohmic heating by Hall current in magnetized capacitively coupled discharges, Plasma Sources Sci. Technol. **28**, 09LT03 (2019).
[43] M. M. Turner, A. Derzsi, Z. Donkó, D. Eremin, S. J. Kelly, T. Lafleur, and T. Mussenbrock, Simulation benchmarks for low-pressure plasmas: Capacitive discharges, Phys. Plasmas **20**, 013507 (2013).
[44] M. Daksha, A. Derzsi, S. Wilczek, J. Trieschmann, T. Mussenbrock, P. Awakowicz, Z. Donkó, and J. Schulze, The effect of realistic heavy particle induced secondary electron emission coefficients on the electron power absorption dynamics in single- and dual-frequency capacitively coupled plasmas, Plasma Sources Sci. Technol. **26**, 085006 (2017).
[45] P. Belenguer and J. P. Boeuf, Transition between different regimes of rf glow discharges, Phys. Rev. A **41**, 4447 (1990).
[46] T. Lafleur, P. Chabert, and J. P. Booth, Electron heating in capacitively coupled plasmas revisited, Plasma Sources Sci. Technol. **23**, 035010 (2014).
[47] T. Lafleur and P. Chabert, Is collisionless heating in capacitively coupled plasmas really collisionless?, Plasma Sources Sci. Technol. **24**, 044002 (2015).
[48] J. Schulze, Z. Donkó, T. Lafleur, S. Wilczek, and R. P. Brinkmann, Spatio-temporal analysis of the electron power absorption in electropositive capacitive RF plasmas based on moments of the Boltzmann equation, Plasma Sources Sci. Technol. **27**, 055010 (2018).
[49] M. Surendra and M. Dalvie, Moment analysis of rf parallel-plate-discharge simulations using the particle-in-cell with Monte Carlo collisions technique, Phys. Rev. E **48**, 3914 (1993).
[50] R. P. Brinkmann, Electron heating in capacitively coupled RF plasmas: A unified scenario, Plasma Sources Sci. Technol. **25**, 014001 (2015).
[51] Y. Fu, B. Zheng, D.-Q. Wen, P. Zhang, Q. H. Fan, and J. P. Verboncoeur, High-energy ballistic electrons in low-pressure radio-frequency plasmas, Plasma Sources Sci. Technol. **29**, 09LT01 (2020).
[52] R. Woo and A. Ishimaru, A similarity principle for multipacting discharges, J. Appl. Phys. **38**, 5240 (1967).
[53] E. Buckingham, On physically similar systems; illustrations of the use of dimensional equations, Phys. Rev. **4**, 345 (1914).
[54] G. J. Hagelaar, Z. Donko, and N. Dyatko, Modification of the Coulomb Logarithm due to Electron-Neutral Collisions, Phys. Rev. Lett. **123**, 25004 (2019).
[55] M. A. Lieberman, J. P. Booth, P. Chabert, J. M. Rax, and M. M. Turner, Standing wave and skin effects in large-area, high-frequency capacitive discharges, Plasma Sources Sci. Technol. **11**, 283 (2002).
[56] K. Zhao, D.-Q. Wen, Y.-X. Liu, M. A. Lieberman, D. J. Economou, and Y. N. Wang, Observation of Nonlinear Standing Waves Excited by Plasma-Series-Resonance-Enhanced Harmonics in Capacitive Discharges, Phys. Rev. Lett. **122**, 185002 (2019).
[57] A. Proto and J. T. Gudmundsson, Electron power absorption in radio frequency driven capacitively coupled chlorine discharge, Plasma Sources Sci. Technol. **30**, 065009 (2021).
[58] J. T. Gudmundsson and A. Proto, Electron heating mode transitions in a low pressure capacitively coupled oxygen discharge, Plasma Sources Sci. Technol. **28**, 045012 (2019).
[59] J. Schulze, A. Derzsi, K. Dittmann, T. Hemke, J. Meichsner, and Z. Donkó, Ionization by Drift and Ambipolar Electric Fields in Electronegative Capacitive Radio Frequency Plasmas, Phys. Rev. Lett. **107**, 275001 (2011).